International Journal of Electrical and Computer Engineering (IJECE)
Vol. 7, No. 5, October 2017, pp. 2555~2564
ISSN: 2088-8708, DOI: 10.11591/ijece.v7i1.pp2555-2564

SVM Classification of MRI Brain Images for Computer-Assisted Diagnosis

Madina Hamiane[1], Fatema Saeed[2]
Department of Telecommunication Engineering, Ahlia University, Manama, Bahrain

Article Info

Article history:

Received Oct 22, 2016
Revised Jan 11, 2017
Accepted Jul 26, 2017

Keyword:

Discrete wavelet transform
support vector machine
Classifier
Feature extraction
MRI brain image processing
Image segmentation

ABSTRACT

Magnetic Resonance Imaging is a powerful technique that helps in the diagnosis of various medical conditions. MRI Image pre-processing followed by detection of brain abnormalities, such as brain tumors, are considered in this work. These images are often corrupted by noise from various sources. The Discrete Wavelet Transforms (DWT) with details thresholding is used for efficient noise removal followed by edge detection and threshold segmentation of the denoised images. Segmented image features are then extracted using morphological operations. These features are finally used to train an improved Support Vector Machine classifier that uses a Gausssian radial basis function kernel. The performance of the classifier is evaluated and the results of the classification show that the proposed scheme accurately distinguishes normal brain images from the abnormal ones and benign lesions from malignant tumours. The accuracy of the classification is shown to be 100% which is superior to the results reported in the literature.

Corresponding Author:

Madina Hamiane
Departement of Telecommunication Engineering,
Ahlia University, Manama, Kingdom of Bahrain
Email: mhhamiane@ahlia.edu.bh

1. INTRODUCTION

In the field of medicine, medical Image processing and analysis has excessive significance. It has arisen as one of the greatest significant tools to detect as well as identify many disorders. It enables both doctors and radiologists to reach a specific diagnosis, by visualizing and analyzing the image.

Computer-Aided Diagnosis (CAD) is a method that is gaining importance in the day-to-day life. It can help radiologists precisely read images and detect probable findings to avoid improper understanding of lesions. However, it is essential to point out that CAD systems can only provide a second opinion and can by no means replace radiologists or physicians.

There are many imaging techniques for the human soft tissue anatomy, such as Computed Tomography (CT), mammogram function, Magnetic Resonance Imaging (MRI) and so on. The focus of this work is on MRI images. MRI is a medical imaging technique that takes images of the inside of the human body. It is a pain-free, non-aggressive, non-radioactive technique for visualizing detailed information regarding the tumors and abnormalities without any human involvement.

In digital image processing, image de-noising is an important procedure to obtain quality images, and enhance and recover detailed information that might be hidden in the data. It removes the noise that is acquired by the image during its acquisition or transmission. This noise is an obstacle for efficient image processing since it gives a poor image quality. Medical images are also corrupted by noise that lowers the visibility of low contrast objects and creates undesirable visual quality. The de-noising process facilitates the image classification accuracy and enhances the medical diagnosis.

The objective of this work is to provide an automatic diagnostic tool that will help medical practitioners in diagnosing brain lesions by distinguishing them from normal brain tissue. The first step is to

enhance the MRI Images by developing their appearance and removing the unusual patterns caused by noise from the interference of different sources. This will result in an alternative image with enhanced and more noticeably structures. The second part of this work is to extract important image features from the de-noised images and use these image characteristics in the classification of the MRI images. This will assist the medical specialist in the interpretation of MRI Brain images.

2. METHODOLOGY AND RESULTS

2.1. Image Database:

MRI brain images used in this work were selected from Harvard Medical School Database [1] which is a web-based database that contains a large variety of MRI brain slice images. The datasets used in this work consists of T2-weighted MRI brain images in axial plane. T2 model was chosen in this work since T2 images are of higher-contrast and clearer vision compared to other modalities.

The number of MRI brain images in the input dataset is Forty. Twenty are of which are normal brain images and twenty of abnormal brain images. The abnormal brain MR images of the dataset consist of the following diseases: Acute stroke, Alzheimer's disease, Cerebral Toxoplasmosis, Chronic subdural hematoma, Hypertensive encephalopathy, Lyme encephalopathy, Metastatic bronchogenic carcinoma, Multiple sclerosis, Sarcoma, Sub-acute stroke, Multiple embolic infarctions, Fatal stroke, Motor neuron disease, Pick's disease and Herpes encephalitis.

2.2. Pre-Processing: MRI Image denoing

The Discrete Wavelet Transforms (DWT) decomposition was used along with thresholding techniques [2] for efficient noise removal. The MATLAB wavelet toolbox was used for this purpose. The wavelet–based methods used for denoising are depicted in Figure 1 below and can be summarized as:

- Decompose: Choose a wavelet and a decomposition level N. Compute the wavelet decomposition of the image down to level N.
- Threshold detail coefficients: For each level from 1 to N, threshold the detail coefficients.
- Reconstruct: Compute wavelet reconstruction using the original approximation coefficients of level N and the modified detail coefficients of levels from 1 to N.

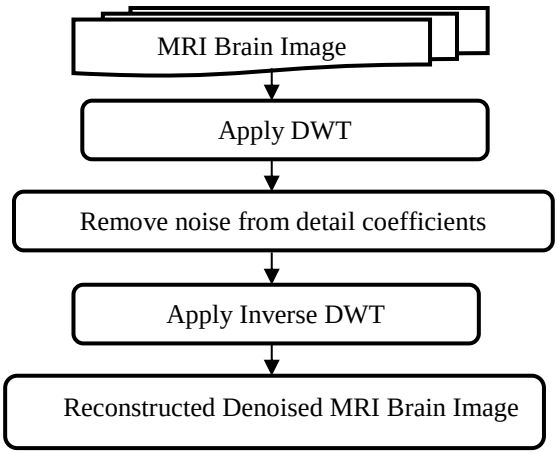

Figure 1. Wavelet Image Denoising

After decomposing the original image that is shown in Figure 2, into its approximation and detail coefficients as shown in Figure 3, all the detail coefficients (Horizontal, diagonal and vertical details) of each level are thresholded according to a thresholding method and a thresholding value. Different threshold methods and different threshold selection values available in MATLAB DWT toolbox were compared. The threshold methods available are: Hard and Soft threshold, while the threshold selection values are: Fixed form threshold, Penalize high, Penalize medium, Penalize low and Bal. sparsity-norm (sqrt). The noise corrupting the images was assumed to be white and thus the available structure of unscaled white noise was considered for the test experiments of this work.

After denoising, the thresholded detail coefficients these were used together with the original approximation coefficient to reconstruct the denoised image as shown in Figure. 4. The effectiveness of the denoising process is measured through the use of the three metrics: Peak Signal to Noise Ratio (PSNR), Signal to Noise Ratio (SNR) and the Mean Squared Error (MSE) [3]-[5].

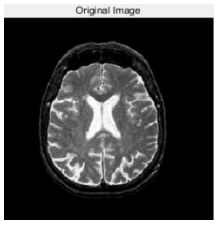

Figure 2. Original MRI brain image

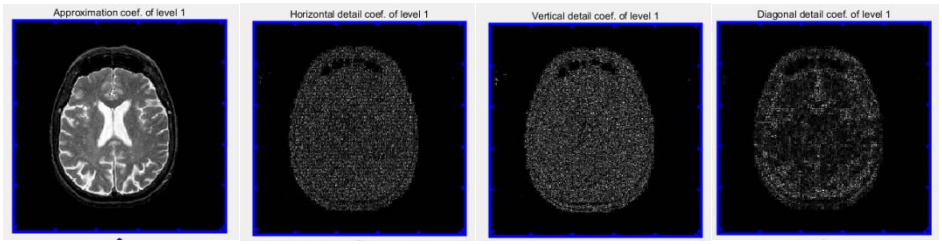

Figure 3. Approximation and detail coefficients

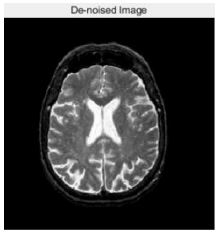

Figure 4. Denoised image

The de-noising is considered effective when the highest values of PSNR and SNR and the lowest value of MSE are reached concurrently. The values of MSE, SNR and PSNR obtained from denoising a sample normal MRI brain image by applying DWT approach with different wavelet types and thresholding techniques are shown in Table 1, Table 2, Table 3 and Table 4. The wavelet types that were used are: Haar, Daubechies (db2 and db4), Symlet (sym2 and sym4), Coiflet (coif1), Biorthogonal (bior1.1, bior3.1, rbio1.1) and dmey. The values in these tables result from the application of soft and hard thresholding to the details of the first and second DWT level decomposition of the image.

Comparisons between the de-noising results in terms of the computed values of MSE, SNR and PSNR obtained when applying hard and soft thresholds on the detail coefficients resulting from the first and second level DWT decomposition of the normal brain images indicate that hard thresholding Is better than soft thresholding in the first and second levels of DWT. In addition, the comparison between the first and second level metrics values obtained with hard thresholding of the details gave better results in the first level of the DWT decomposition, especially with the selection threshold value method of Bal. sparsity-norm (sqrt).

Table 1. Soft Threshold of the First Level DWT

	Fixed Form Threshold			Bal. sparsity-norm (sqrt)		
	MSE	SNR	PSNR	MSE	SNR	PSNR
haar	6.8441	28.6988	39.7776	6.2676	29.081	40.1598
db2	7.0249	28.5856	39.6644	12.2775	26.1609	37.2397
db4	7.1624	28.5014	39.5802	14.5285	25.4298	36.5086
sym2	7.0249	28.5856	39.6644	12.2775	26.1609	37.2397
sym4	7.0913	28.5447	39.6235	12.3006	26.1527	37.2315
coif1	7.0695	28.5581	39.6369	12.4009	26.1175	37.1963
bior1.1	6.8441	28.6988	39.7776	6.2676	29.081	40.1598
bior3.1	7.2066	28.4747	39.5535	12.5871	26.0527	37.1316
rbio1.1	6.8441	28.6988	39.7776	6.2676	29.081	40.1598
dmey	8.4339	27.7917	38.8705	12.3989	26.1182	37.197

Table 2. Hard Threshold of the First Level DWT

	Fixed Form Threshold			**Bal. sparsity-norm (sqrt)**		
	MSE	SNR	PSNR	MSE	SNR	PSNR
Haar	6.0745	29.2169	40.2957	**6.0552**	**29.2307**	**40.3095**
db2	6.0687	29.221	40.2998	6.1166	29.1869	40.2657
db4	6.0973	29.2006	40.2794	6.241	29.0994	40.1782
sym2	6.0687	29.221	40.2998	6.1166	29.1869	40.2657
sym4	6.0984	29.1998	40.2787	6.1783	29.1433	40.2221
coif1	6.0979	29.2002	40.279	6.1894	29.1355	40.2143
bior1.1	6.0745	29.2169	40.2957	**6.0552**	**29.2307**	**40.3095**
bior3.1	6.1221	29.183	40.2618	6.2461	29.0959	40.1747
rbio1.1	6.0745	29.2169	40.2957	**6.0552**	**29.2307**	**40.3095**
dmey	6.1068	29.1938	40.2727	6.1981	29.1294	40.2082

Table III. Soft threshold of the Second level DWT

	Fixed Form Threshold			**Bal. sparsity-norm (sqrt)**		
	MSE	**SNR**	**PSNR**	**MSE**	**SNR**	**PSNR**
haar	7.5359	28.2806	39.3595	16.1744	24.9637	36.0425
db2	7.6185	28.2333	39.3121	17.7031	24.5715	35.6503
db4	7.5661	28.2633	39.3421	17.7031	24.8113	35.6503
sym2	7.6185	28.2333	39.3121	17.7031	24.5715	35.6503
sym4	7.642	28.2199	39.2987	18.0929	24.4769	35.5557
coif1	7.6258	28.2291	39.3079	20.0744	24.0256	35.1044
bior1.1	7.5359	28.2806	39.3595	16.1744	24.9637	36.0425
bior3.1	7.9474	28.0498	39.1286	11.7208	26.3624	37.4412
rbio1.1	7.5359	28.2806	39.3595	16.1744	24.9637	36.0425
dmey	7.646	28.2176	39.2964	16.632	24.8425	35.9214

The Penalize high, medium and low method does not differentiate significantly between the different decomposition levels, the different wavelets and between the thresholding methods as it gave the same metrics values for all wavelets and both levels of DWT decomposition as well as the same metrics values for hard and soft thresholding methods. We can therefore conclude that this thresholding technique is not suitable for denoising of MRI brain images that were used in this work and was discarded from the analysis.

The first level of DWT denoising with hard thresholding and with the "Bal. sparsity-norm (sqrt)" techniques of thresholding gave the best results. Since the same results were obtained for the Haar, Bior and Rbio wavelets, the denoising process was thus repeated for the members of the same wavelets and the results were tabulated in Table 5 which indicates that inBior1.3 gave the minimum MSE, highest SNR and highest PSNR values for the five images compared to other wavelet members.

Table 4. Hard Threshold of the Second Level DWT

	Fixed Form Threshold			**Bal. sparsity-norm (sqrt)**		
	MSE	SNR	PSNR	MSE	SNR	PSNR
haar	**6.1712**	**29.1483**	**40.2271**	6.6652	39.8927	39.8927
db2	6.2036	29.1255	40.2044	8.3351	27.8429	38.9217
db4	6.2313	29.1062	40.185	8.5546	27.73	38.8088
sym2	6.2036	29.1255	40.2044	8.3351	27.8429	38.9217
sym4	6.2315	29.1061	40.1849	8.7586	27.6276	38.7065
coif1	6.2027	29.1262	40.205	9.0768	27.4727	38.5515
bior1.1	**6.1712**	**29.1483**	**40.2271**	6.6652	28.8139	39.8927
bior3.1	6.4499	28.9564	40.0353	7.4515	28.3296	39.4084
rbio1.1	**6.1712**	**29.1483**	**40.2271**	6.6652	28.8139	39.8927
dmey	6.2565	29.0887	40.1675	8.4553	27.7807	38.8595

Table 5. Hard threshold of the First Level DWT with Bal. Sparsity-Norm (sqrt) Method

	Bal. sparsity-norm (sqrt)		
	MSE	**SNR**	**PSNR**
bior1.1	6.0552	29.2307	40.3095
bior1.3	**6.0511**	**29.2336**	**40.3124**
bior1.5	6.0534	29.232	40.3108
bior2.2	6.1998	29.1282	40.207
bior2.4	6.1978	29.1296	40.2084
bior2.6	6.1977	29.1296	40.2085
bior2.8	6.1899	29.1352	40.214
bior3.1	6.2461	29.0959	40.1747
bior3.3	6.2464	29.0957	40.1745
bior3.5	6.2165	29.1165	40.1953
bior3.7	6.2159	29.1169	40.1958
bior3.9	6.2118	29.1198	40.1987
bior4.4	6.1719	29.1478	40.2266
bior5.5	6.1773	29.144	40.2228
bior6.8	6.1902	29.1349	40.2137
rbio1.1	6.0552	29.2307	40.3095
rbio1.3	6.1013	29.1977	40.2766
rbio1.5	6.1116	29.1904	40.2693
rbio2.2	6.172	29.1477	40.2265
rbio2.4	6.1801	29.1421	40.2209
rbio2.6	6.173	29.147	40.2258
rbio2.8	6.1859	29.138	40.2168
rbio3.1	6.6033	28.8544	39.9332
rbio3.3	6.3139	29.049	40.1278
rbio3.5	6.2597	29.0865	40.1653
rbio3.7	6.2472	29.0951	40.1739
rbio3.9	6.2441	29.0973	40.1761
rbio4.4	6.2302	29.107	40.1858
rbio5.5	6.2321	29.1057	40.1845
rbio6.8	6.1859	29.138	40.2168

After testing the above procedure on all normal brain images and identifying the best wavelet type, best DWT level along with the best thresholding technique, based on the above metrics, the same procedure of denoising was applied to all MRI brain images in the input data set.

2.3. Image Segmentation

Image segmentation is a method that split an image to a group of non-overlapping areas [6] .The unification of these areas is the whole image. However, the boundaries of various tissues in brain images are unclear and the intensities of the gray and white tissues are almost similar. The adjacent tissues are difficult to be separated because the boundaries are smooth and the intensity does not change too much between these tissues. Hence, edge detection is required prior to the image segmentation.

Image edges were detected by using the Canny method to find the binary gradient mask [7] as shown in Figure 5. To detect weak and strong edges, this method uses two thresholds. Hence, the Canny method is more likely to detect true weak edges, and less likely than the other methods to be dispersed by noise. After detecting the edges, these edges were outlined on the original image to differentiate between different tissues of the brain.

After outlining the edges on the image, global threshold using Otsu's method [8] was applied to identify the intensity level, and the image was then converted to a binary image and thresholded according to

value returned by the function of Otsu's method. An example of the threshold segmentation output is shown in Figure 6.

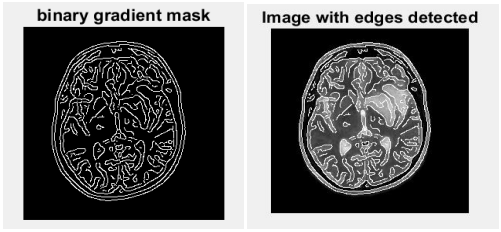

Figure 5. Binary gradient mask and abnormal brain with edges detected

Figure 6. Threshold Segmentation

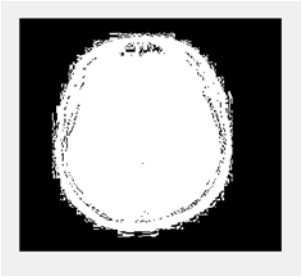

Figure 7. Threshold Segmentation without Edge Detection

The thresholded image obtained by applying Otsu's threshold but without edge detection is shown in Figure 7. and clearly indicates that the edge detection technique is an important step that should not be suppressed when applying the segmentation step that is based on intensity thresholding.

Figure 8. Tumor Threshold Mask

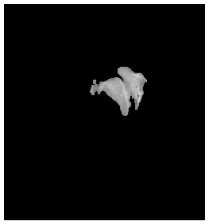

Figure 9. Extracted Tumor Image

After thresholding the image, the holes in the image that are the same as the background were filled. The thresholded image was then converted to a binary image and morphological operations were applied to remove isolated pixels which are individual 1s that are surrounded by 0s. Next, another morphological operation was applied that performs erosion followed by dilation. Erosion removes pixels on object boundaries while dilation adds pixels to the boundaries of objects in an image. The regions of interest (ROI) were subsequently extracted from the binary image as shown in Figure 8 displaying a tumor mask. The tumor was extracted from the brain image by assigning a value of 0 to all pixels except the pixels of the tumor mask as shown in Figure 9.

2.4. Image Feature Extraction

Various techniques for extracting features from MRI brain images have been reported in the literature, the most common are: Discrete Wavelet Transform (DWT) [9] , Gabor filters [10] and Gray Level Co-occurrence Matrix (GLCM) [11]. Both DWT and Gabor Filter methods produce feature vectors with a large number of elements which necessitates the use of size reduction techniques prior to feeding the feature vectors to the classifier. On the other hand, The Gray Level Co-occurrence Matrix (GLCM) has proven to be

superior in terms the dimension of the feature vectors and thus is more appropriate for MRI image classification.

GLCM is a statistical technique for extracting texture features from images [11]. It assumes that the texture of normal tissues is very different from the texture of tumor tissues. The texture features extracted from the GLCM matrix are: contrast, correlation, energy, homogeneity. Selecting a good set of features improve the process of classification. Additional features were also extracted from this matrix which are: mean, standard deviation, entropy, root mean square, variance, kurtosis, skewness. All features used in this work are listed in Table 6. These features were extracted from the twenty normal images forming class I images and the thirty images of abnormal regions of interest forming class II images. The averaged features values are shown in Table 7.

Table 6. GLCM Features

Features	Equation
Contrast	$\sum_{i,\ j=0}^{N-1} p(i,j)\lvert i-j\rvert^2$
Correlation	$\frac{\sum_i \sum_j [ij\ p(i,j)] - \alpha_i \alpha_j}{p_i p_j}$
Energy	$\sum_{i,\ j=0}^{N-1} p(i,j)^2$
Homogeneity	$\sum_i \sum_j \frac{p(i,j)}{1+\lvert i+j\rvert}$
Mean	$\frac{\sum_{i,\ j}^{N-1} p(i,j)}{N-1}$
Standard deviation	$\sqrt{\frac{1}{N}\sum_{i=1}^{N}(x_i-\mu)^2}$
Entropy	$-\sum_i \sum_j p(i,j) \ln p(i,j)$
RMS	$\sqrt{\frac{1}{N}\sum_{n=1}^{N}\lvert X_n\rvert^2}$
Variance	$\sum_i^{N-1}\sum_j^{N-1}(i-\mu)^2\, p(i,j)$
Kurtosis	$n = \frac{\sum_{i=1}^{n}(X_i - X_{avg})^4}{(\sum_{i=1}^{n}(X_i - X_{avg})^2)^2}$
Skewness	$\sqrt{n}\ \frac{\sum_{i=1}^{n}(X_i - X_{avg})^3}{(\sum_{i=1}^{n}(X_i - X_{avg})^2)^{3/2}}$

Table 7. Extracted features of normal and abnormal images

Class/Feature	Class I (Normal)	Class I (Abormal)
Contrast	0.16178	0.053002
Correlation	0.96945	0.95696
Energy	0.482798	0.935961
Homogeneity	0.95239	0.99253
Mean	4088	1020
Standard Deviation	22527.972	7888.474
Entropy	0.457085	0.923
RMS	10606.13	2854.718
Variance	5.13E+08	62293236
Kurtosis	59.01666	61.9667
Skewness	7.533646	7.806567

2.5. Image Classification

Classification is the process of categorizing a given input by a proper classifier. The objective of classification is to give a label to each MR brain image based on some image's features. The structure layout and design of a classification system involves the choice and calculation of features from the images that we want to classify as shown in Figure 10 [6].

Support Vector Machine (SVM) classifier was used in this work as it has shown to result in greater accuracy compared to other classifier structures in the classification of MRI images [12] - [13]. The Support Vector Machine (SVM) is a supervised learning technique that uses a set of labelled training data as input to train the classifier and produce input-output mapping functions.

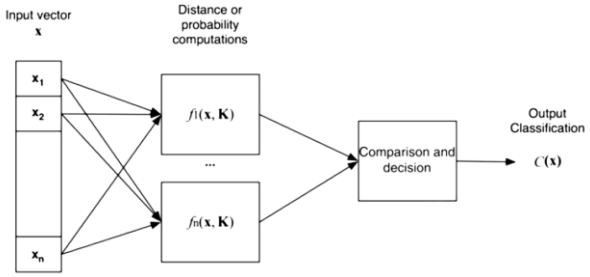

Figure 10. Image Classification System structure [6]

For MRI images, the SVM output is a hyperplane that classifies new MRI images. For the case of the two class-classification used in this work, the process of the SVM technique is to find the hyperplane that provides the largest minimum distance to the training data as shown in Figure 11. [14]-[15]

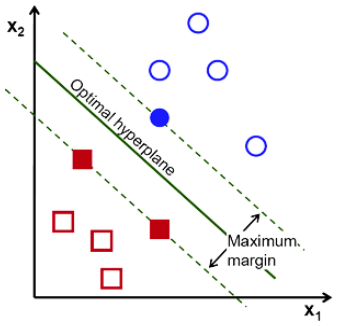

Figure 11. Optimal hyperplane in SVM [15]

The SVM classifier used in this work provides the possibility of choosing the kernel function [13]. The kernel function chosen is 'RBF' that represents the Gaussian Radial Basis Function kernel. This choice was based on the excellent performance of this SVM kernel function as reported in the literature. The input data set was divided in two subsets, a training set consisting of ten normal images and fifteen abnormal images and a testing set consisting of the remaining ten normal and fifteen abnormal images. The Support Vector Machine (SVM) classifier was trained after extracting the features and labels from the training set.

After training the classifier, the testing set was used to test the performance of the classifier and its ability to accurately classify the MRI images as either normal or abnormal. To evaluate our SVM classifier, a confusion matrix was built as shown in Table 8. and the performance of the classifier evaluated as shown in Table IX. In the testing test, ten images were labelled as Normal and the remaining fifteen images were labelled as Abnormal. As indicated in Table 9, the classifier succeeded to classify MRI brain images into normal and abnormal.

Table 8. Confusion Matrix

		Predicted	
		Normal	**Abnormal**
Truth	**Normal**	20	0
	Abnormal	0	30

Table 9. Performance of RBF SVM classifier

Classes	No. of images classified	No. of images misclassified	Sensitivity	specificity	Accuracy
Class I (Normal)	20	0	100%	100%	100%
Class II (Abnormal)	30	0	100%	100%	100%

3. SUMMARY OF RESULTS

In this work, the two dimensional wavelet toolbox of MATLAB was used for the pre-processing of the images by applying DWT to remove the noise from MRI brain images. The process first decomposes the image, then applies threshold to the detail coefficients and after that reconstructs the noise-free image. Different wavelets, thresholding techniques with various threshold selection types were investigated to choose the best wavelet type and decomposition level along with the best thresholding technique. The evaluation was done based on the values of the three metrics MSE, SNR and PSNR. Bior1.3 wavelet has proven to be the best wavelet along with the first level of decomposition, hard thresholding and Bal. sparsity-norm (sqrt) as the method of threshold selection value. Bior1.3 wavelet was applied on all images that were used in this work.

MATLAB functions from the Image processing and the bioinformatics toolboxes were then used in the image processing phase. Edge detection was applied as the first step to detect the edges of MRI brain images. Canny method was then used which gave very good results. The edges were outlined on the original image to differentiate between the various tissues of the brain, and then the brain images were segmented based on intensity segmentation by using Otsu's method as a second step. The last step of image processing was to apply the morphological operations of erosion and dilation to extract the region of interest.

The steps used in processing the MRI brain images have shown effective extraction of the region of interest from the twenty normal and thirty abnormal images. The extracted region of interest was then used in the post processing step for the extraction of their features. GLCM was used to create a gray level co-occurrence matrix from images. GLCM yielded 11 distinct features that were subsequently used in the classification step. The features were extracted from each of the fifty brain images to form the feature matrix characterising the image. Classification was performed using Support Vector machine with Gaussian Radial Basis Function kernel which resulted in an effective classification of all images with 100% accuracy.

4. CONCLUSION

MRI images have many advantages in biomedical engineering compared to other imaging techniques. This work focused on brain images because large areas of the organ process are affected by brain injuries. Most movement and body functions are controlled and coordinated by the brain.

De-noising of MRI brain images was one of the objectives of this work. It was found that MRI brain images can be efficiently denoised using the Discrete Wavelet Transforms (DWT) with thresholding as confirmed by the optimal metrics values obtained. Further enhancement of the images was obtained through the use of edge detection and threshold segmentation. It was shown that elimination of the edge detection step resulted in segmentation inaccuracies. In addition, morphological operations were used to extract the region of interest in the image.

Several features were extracted from the enhanced MRI images and were used to train an SVM classifier with RBF kernel which succeeded in classifying the MRI brain images as normal or abnormal. The accuracy of the SVM model was found to be 100% which outperforms results reported in the literature. This accurate classification of the SVM classifier can be used by neurologists to help them to identify the abnormality that might be hidden, due to the large number of slices that are obtained from MRI brain images.

REFERENCES

[1] K. & Becker J., The Whole Brain Atlas [http://www. med.harvard .edu/ aanlib/home.html]
[2] A. Dixit, & P. Sharma, "A Comparative Study of Wavelet Thresholding for Image Denoising", *International Journal of Image, Graphics and Signal Processing*, 39-46., 2014.
[3] A. Georg, & A. Prabavathy, "A Survey On Different Approaches Used In Image Quality Assessment", *International Journal of Emerging Technology and Advanced Engineering*, Volume 3, Issue 2, 2013.
[4] C. Varnan, A. Jagan, J. Kaur, D. Jyoti, & D. Rao, "Image Quality Assessment Techniques pn Spatial Domain", *International Journal of Computer Science and Technology*, Vol. 2, Issue 3 , 2011.
[5] S. Nisha, "Image Quality Assessment Techniques", *International Journal of Advanced Research in Computer Science and Software Engineering*, Volume 3, Issue 7, 2013.

[6] O. Marques, Practical Image and Video Processing Using MATLAB, by John Wiley & So"ns, Inc.,2011.
[7] A. Kulkarni, & R. Kamathe, "MRI Brain Image Segmentation by Edge Detection and Region Selection", *International Journal of Technology and Science*, Issue. 2, Vol. 1, 2014
[8] G. Evelin Sujji ,Y.V.S.Lakshmi, & G. Wiselin Ji, "MRI Brain Image Segmentation based on Thresholding", *International Journal of Advanced Computer Research*, Vol. 3, No.1 , Issue 8 , 2013.
[9] Icke, Guzide, Kamarthi, V.Sagar , "Feature extraction through discrete wavelet transform coefficients", *Intelligent Systems in Design and Manufacturing VI, Proceedings of the SPIE*, Volume 5999, pp. 27-35, 2005.
[10] S. Shah, & N Chauhan, "Classification of Brain MRI Images using Computational Intelligent Techniques", *International Journal of Computer Applications*, Volume 124 , No.14. 2015.
[11] Zulpe, N. & Pawar, V., "GLCM Textural Features for Brain Tumor Classification", *International Journal of Computer Science Issues*, Vol. 9, Issue 3, No 3, 2012
[12] V. Josephine, & P. Latha, "SVM -Based Automatic Medical Decision Support System For Medical Image", *Journal of Theoretical and Applied Information Technolog*, Vol. 66 No.3., 2014.
[13] A Yuniarti, "Classification and numbering of dental radiographs for an automated human identification system," *TELKOMNIKA Telecommunication, Computing, Electronics and Control.*, vol. 10, no. 1, pp. 137-146, 2012.
[14] D. Boswell, Introduction to Support Vector Machines, available at: http://dustwell.com/PastWork/Intro ToSVM .pdf
[15] OpenCV, Introduction to Support Machines, available at: http://docs.opencv.org/2.4/doc/tutorials/ml/introductio _to_svm/introduction_to_svm.html